

We are IntechOpen, the world's leading publisher of Open Access books Built by scientists, for scientists

6,900

Open access books available

186,000

International authors and editors

200M

Downloads

Our authors are among the

154

Countries delivered to

TOP 1%

most cited scientists

12.2%

Contributors from top 500 universities



WEB OF SCIENCE™

Selection of our books indexed in the Book Citation Index
in Web of Science™ Core Collection (BKCI)

Interested in publishing with us?
Contact book.department@intechopen.com

Numbers displayed above are based on latest data collected.
For more information visit www.intechopen.com



Light Cold Dark Matter in a Two-Singlet Model

Abdessamad Abada and Salah Nasri

Additional information is available at the end of the chapter

<http://dx.doi.org/10.5772/52243>

1. Introduction

Understanding the nature of dark matter (DM) as well as the origin of baryon asymmetry are two of the most important questions in both Cosmology and Particle Physics. The failure of the Standard Model (SM) of the electroweak and strong interactions in accommodating such questions motivates the search for an explanation in the realm of new physics beyond it. The most attractive strategy so far has been to look into extensions of the SM that incorporate electrically neutral and colorless weakly interacting massive particles (WIMPs), with masses from one to a few hundred GeV, coupling constants in the milli-weak scale and lifetimes longer than the age of the Universe.

The most popular extension of the SM is the minimal supersymmetric standard model (MSSM) in which the neutral lightest supersymmetric particle (LSP) is seen as a candidate for dark matter. Indeed, neutralinos are odd under R -parity and are only produced or destroyed in pairs, thus making the LSP stable [1]. They can annihilate through a t -channel sfermion exchange into Standard Model fermions, or via a t -channel chargino-mediated process into W^+W^- , or through an s -channel pseudoscalar Higgs exchange into fermion pairs. They can also undergo elastic scattering with nuclei through mainly a scalar Higgs exchange [2].

However, most particularly in light of the recent signal reported by CoGeNT [3], which favors a light dark matter (LDM) with a mass in the range 7 – 9 GeV and nucleon scattering cross section $\sigma_{\text{det}} \sim 10^{-4}$ pb, having a neutralino as a LDM candidate can be challenging. Indeed, systematic studies show that an LSP with a mass around 10 GeV and an elastic scattering cross-section off a nucleus larger than $\sim 10^{-5}$ pb requires a very large $\tan \beta$ and a relatively light CP-odd Higgs [4]. This choice of parameters leads to a sizable contribution to the branching ratios of some rare decays, which then disfavors the scenario of light neutralinos [5]. Also, in the next-to-minimal supersymmetric standard model (NMSSM) with 12 input parameters [6], realizing a LDM with an elastic scattering cross section capable of generating the CoGeNT signal is possible only in a finely-tuned region of the parameters where the neutralino is mostly singlino and the light CP-even Higgs is singlet-like with a mass below a few GeV. In such a situation, it is very difficult to detect such a light Higgs at the collider. It is clear then that other alternative scenarios for LDM are needed [7].

The simplest of scenarios is then to extend the Standard Model by a real \mathbb{Z}_2 symmetric scalar field, the dark matter, which has to be a SM gauge singlet that interacts with visible particles via the Higgs field only. Such an extension was first proposed in [8] and further studied in [9] where the \mathbb{Z}_2 symmetry is extended to a global U(1) symmetry, more extensively in [10]. Specific implications on Higgs detection and LHC physics were discussed in [11] and one-loop vacuum stability and perturbativity bounds discussed in [12]. However, the work of [13] uses constraints from the experiments XENON10 [14] and CDMSII [15] to exclude DM masses smaller than 50, 70 and 75 GeV for Higgs masses equal to 120, 200 and 350 GeV respectively. Also, the Fermi-LAT data on the isotropic diffuse gamma-ray emission can potentially exclude this one-singlet dark-matter model for masses as low as 6 GeV, assuming a NFW profile for the dark-matter distribution [16].

Therefore, a two-singlet extension of the Standard Model was proposed in [17] as a simple model for light cold dark matter. Both scalar fields are \mathbb{Z}_2 symmetric with one undergoing spontaneous symmetry breaking. The behavior of the model under the DM relic-density constraint and the restrictions from experimental direct detection was studied. It was concluded that the model was capable of bearing a light dark-matter WIMP.

The present chapter describes how we can further the study of the two-singlet scalar model (2SSM) by discussing some of its phenomenological implications. We limit ourselves to small DM masses, from 0.1 GeV to 10 GeV. We discuss the implications of the model on the meson factories and the Higgs search at the LHC. In fact, it is pertinent at this stage to mention that there are more than one motivation for scalar-singlet extensions of the SM. Indeed, besides providing a possible account for the dark matter in the Universe consistent with the CoGeNT signal, they also provide a solution to the mu problem in the supersymmetric standard model. They can explain the matter-anti matter asymmetry in the Universe [18], and account for the possible occurrence of a light Higgs with a mass less or equal to 100 GeV while still in agreement with the electroweak precision tests [19] and potential signatures at *B*-factories [20].

This chapter is organized as follows. The next section introduces briefly the model and summarizes the results of [17] regarding relic-density constraint and direct detection. The two following sections investigate the rare decays of *Y* (section three) and *B* (section four) mesons, most particularly their invisible channels. Section five looks into the decay channels of the Higgs particle. In each of these situations, we try, when possible, to deduce preferred regions of the parameter space and excluded ones. The last section is devoted to concluding remarks. Results presented here are found in [20].

2. The 2SSM Model

The Standard Model is extended with two real, spinless and \mathbb{Z}_2 -symmetric fields. One is the dark-matter field S_0 with unbroken symmetry to ensure the stability of the dark matter, the other is an auxiliary field χ_1 for which the symmetry is spontaneously broken. Both fields are Standard-Model gauge singlets and can interact with SM particles only via the Higgs doublet H . This latter is taken in the unitary gauge such that $H^\dagger = 1/\sqrt{2} (0 \ h')$, where h' is a real scalar. We assume all processes calculable in perturbation theory. The potential function that incorporates S_0 , h' and χ_1 is:

$$U = \frac{\tilde{m}_0^2}{2} S_0^2 - \frac{\mu^2}{2} h'^2 - \frac{\mu_1^2}{2} \chi_1^2 + \frac{\eta_0}{24} S_0^4 + \frac{\lambda}{24} h'^4 + \frac{\eta_1}{24} \chi_1^4 + \frac{\lambda_0}{4} S_0^2 h'^2 + \frac{\eta_{01}}{4} S_0^2 \chi_1^2 + \frac{\lambda_1}{4} h'^2 \chi_1^2. \quad (1)$$

The mass parameters squared \tilde{m}_0^2 , μ^2 and μ_1^2 and all the coupling constants are real positive numbers. Electroweak spontaneous symmetry breaking occurs for the Higgs field with the vacuum expectation value $v = 246\text{GeV}$. The field χ_1 will oscillate around the vacuum expectation value v_1 which we take at the electroweak scale 100GeV . Writing $h' = v + \tilde{h}$ and $\chi_1 = v_1 + \tilde{S}_1$, the potential function becomes, up to an irrelevant zero-field energy:

$$U = U_{\text{quad}} + U_{\text{cub}} + U_{\text{quar}}, \quad (2)$$

where the quadratic terms are given by:

$$U_{\text{quad}} = \frac{1}{2} m_0^2 S_0^2 + \frac{1}{2} M_h^2 \tilde{h}^2 + \frac{1}{2} M_1^2 \tilde{S}_1^2 + M_{1h}^2 \tilde{h} \tilde{S}_1, \quad (3)$$

with the mass-squared coefficients related to the original parameters of the theory by the following relations:

$$\begin{aligned} m_0^2 &= \tilde{m}_0^2 + \frac{\lambda_0}{2} v^2 + \frac{\eta_{01}}{2} v_1^2; & M_h^2 &= -\mu^2 + \frac{\lambda}{2} v^2 + \frac{\lambda_1}{2} v_1^2; \\ M_1^2 &= -\mu_1^2 + \frac{\lambda_1}{2} v^2 + \frac{\eta_1}{2} v_1^2; & M_{1h}^2 &= \lambda_1 v v_1. \end{aligned} \quad (4)$$

Clearly, we need to diagonalize the mass-squared matrix. Denoting the physical mass-squared field eigenmodes by h and S_1 , we rewrite:

$$U_{\text{quad}} = \frac{1}{2} m_0^2 S_0^2 + \frac{1}{2} m_h^2 h^2 + \frac{1}{2} m_1^2 S_1^2, \quad (5)$$

where the physical fields are related to the mixed ones by a 2×2 rotation:

$$\begin{pmatrix} h \\ S_1 \end{pmatrix} = \begin{pmatrix} \cos \theta & \sin \theta \\ -\sin \theta & \cos \theta \end{pmatrix} \begin{pmatrix} \tilde{h} \\ \tilde{S}_1 \end{pmatrix}. \quad (6)$$

Here θ is the mixing angle, given by the relation $\tan 2\theta = 2M_{1h}^2 / (M_1^2 - M_h^2)$, and the physical masses in (5) by the two relations:

$$\begin{aligned} m_h^2 &= \frac{1}{2} \left[M_h^2 + M_1^2 + \varepsilon (M_h^2 - M_1^2) \sqrt{(M_h^2 - M_1^2)^2 + 4M_{1h}^4} \right]; \\ m_1^2 &= \frac{1}{2} \left[M_h^2 + M_1^2 - \varepsilon (M_h^2 - M_1^2) \sqrt{(M_h^2 - M_1^2)^2 + 4M_{1h}^4} \right], \end{aligned} \quad (7)$$

where ε is the sign function.

Written now directly in terms of the physical fields, the cubic interaction terms are expressed as follows:

$$U_{\text{cub}} = \frac{\lambda_0^{(3)}}{2} S_0^2 h + \frac{\eta_{01}^{(3)}}{2} S_0^2 S_1 + \frac{\lambda^{(3)}}{6} h^3 + \frac{\eta_1^{(3)}}{6} S_1^3 + \frac{\lambda_1^{(3)}}{2} h^2 S_1 + \frac{\lambda_2^{(3)}}{2} h S_1^2, \quad (8)$$

where the cubic physical coupling constants are related to the original parameters via the following relations:

$$\begin{aligned} \lambda_0^{(3)} &= \lambda_0 v \cos \theta + \eta_{01} v_1 \sin \theta, \\ \eta_{01}^{(3)} &= \eta_{01} v_1 \cos \theta - \lambda_0 v \sin \theta; \\ \lambda^{(3)} &= \lambda v \cos^3 \theta + \frac{3}{2} \lambda_1 \sin 2\theta (v_1 \cos \theta + v \sin \theta) + \eta_1 v_1 \sin^3 \theta; \\ \eta_1^{(3)} &= \eta_1 v_1 \cos^3 \theta - \frac{3}{2} \lambda_1 \sin 2\theta (v \cos \theta - v_1 \sin \theta) - \lambda v \sin^3 \theta; \\ \lambda_1^{(3)} &= \lambda_1 v_1 \cos^3 \theta + \frac{1}{2} \sin 2\theta [(2\lambda_1 - \lambda) v \cos \theta - (2\lambda_1 - \eta_1) v_1 \sin \theta] - \lambda_1 v \sin^3 \theta; \\ \lambda_2^{(3)} &= \lambda_1 v \cos^3 \theta - \frac{1}{2} \sin 2\theta [(2\lambda_1 - \eta_1) v_1 \cos \theta + (2\lambda_1 - \lambda) v \sin \theta] + \lambda_1 v_1 \sin^3 \theta. \end{aligned} \quad (9)$$

In the same way, in terms of the physical fields too, the quartic interactions are given by:

$$\begin{aligned} U_{\text{quar}} &= \frac{\eta_0}{24} S_0^4 + \frac{\lambda^{(4)}}{24} h^4 + \frac{\eta_1^{(4)}}{24} S_1^4 + \frac{\lambda_0^{(4)}}{4} S_0^2 h^2 + \frac{\eta_{01}^{(4)}}{4} S_0^2 S_1^2 + \frac{\lambda_{01}^{(4)}}{2} S_0^2 h S_1 \\ &\quad + \frac{\lambda_1^{(4)}}{6} h^3 S_1 + \frac{\lambda_2^{(4)}}{4} h^2 S_1^2 + \frac{\lambda_3^{(4)}}{6} h S_1^3, \end{aligned} \quad (10)$$

with the physical quartic coupling constants written as:

$$\begin{aligned} \lambda^{(4)} &= \lambda \cos^4 \theta + \frac{3}{2} \lambda_1 \sin^2 2\theta + \eta_1 \sin^4 \theta, \\ \eta_1^{(4)} &= \eta_1 \cos^4 \theta + \frac{3}{2} \lambda_1 \sin^2 2\theta + \lambda \sin^4 \theta; \\ \lambda_0^{(4)} &= \lambda_0 \cos^2 \theta + \eta_{01} \sin^2 \theta, \\ \eta_{01}^{(4)} &= \eta_{01} \cos^2 \theta + \lambda_0 \sin^2 \theta; \\ \lambda_{01}^{(4)} &= \frac{1}{2} (\eta_{01} - \lambda_0) \sin 2\theta, \\ \lambda_1^{(4)} &= \frac{1}{2} [(3\lambda_1 - \lambda) \cos^2 \theta - (3\lambda_1 - \eta_1) \sin^2 \theta] \sin 2\theta; \\ \lambda_2^{(4)} &= \lambda_1 \cos^2 2\theta - \frac{1}{4} (2\lambda_1 - \eta_1 - \lambda) \sin^2 2\theta; \\ \lambda_3^{(4)} &= \frac{1}{2} [(\eta_1 - 3\lambda_1) \cos^2 \theta - (\lambda - 3\lambda_1) \sin^2 \theta] \sin 2\theta. \end{aligned} \quad (11)$$

Finally, after spontaneous breaking of the electroweak and \mathbb{Z}_2 symmetries, the part of the Standard Model Lagrangian that is relevant to dark matter annihilation writes, in terms of the physical fields h and S_1 , as follows:

$$U_{\text{SM}} = \sum_f \left(\lambda_{hf} h \bar{f} f + \lambda_{1f} S_1 \bar{f} f \right) + \lambda_{hw}^{(3)} h W_\mu^- W^{+\mu} + \lambda_{1w}^{(3)} S_1 W_\mu^- W^{+\mu} \\ + \lambda_{hz}^{(3)} h (Z_\mu)^2 + \lambda_{1z}^{(3)} S_1 (Z_\mu)^2 + \lambda_{hw}^{(4)} h^2 W_\mu^- W^{+\mu} + \lambda_{1w}^{(4)} S_1^2 W_\mu^- W^{+\mu} \\ + \lambda_{h1w} h S_1 W_\mu^- W^{+\mu} + \lambda_{hz}^{(4)} h^2 (Z_\mu)^2 + \lambda_{1z}^{(4)} S_1^2 (Z_\mu)^2 + \lambda_{h1z} h S_1 (Z_\mu)^2. \quad (12)$$

The quantities m_f , m_w and m_z are the masses of the fermion f , the W and the Z gauge bosons respectively, and the above coupling constants are given by the following relations:

$$\lambda_{hf} = -\frac{m_f}{v} \cos \theta; \quad \lambda_{1f} = \frac{m_f}{v} \sin \theta; \\ \lambda_{hw}^{(3)} = 2 \frac{m_w^2}{v} \cos \theta; \quad \lambda_{1w}^{(3)} = -2 \frac{m_w^2}{v} \sin \theta; \\ \lambda_{hz}^{(3)} = \frac{m_z^2}{v} \cos \theta; \quad \lambda_{1z}^{(3)} = -\frac{m_z^2}{v} \sin \theta; \\ \lambda_{hw}^{(4)} = \frac{m_w^2}{v^2} \cos^2 \theta; \quad \lambda_{1w}^{(4)} = \frac{m_w^2}{v^2} \sin^2 \theta; \quad \lambda_{h1w} = -\frac{m_w^2}{v^2} \sin 2\theta; \\ \lambda_{hz}^{(4)} = \frac{m_z^2}{2v^2} \cos^2 \theta; \quad \lambda_{1z}^{(4)} = \frac{m_z^2}{2v^2} \sin^2 \theta; \quad \lambda_{h1z} = -\frac{m_z^2}{2v^2} \sin 2\theta. \quad (13)$$

2.1. Dark Matter relic density constraint

The field S_0 is odd under the unbroken \mathbb{Z}_2 symmetry, and so is a stable relic and can therefore constitute the dark matter of the Universe. Its relic density can be obtained using the standard approximate solutions to the Boltzmann equations [21]:

$$\Omega_D \bar{h}^2 = \frac{1.07 \times 10^9 x_f}{\sqrt{g_*} M_{\text{Pl}} \langle v_{12} \sigma_{\text{ann}} \rangle \text{GeV}}, \quad (14)$$

where \bar{h} is the normalized Hubble constant, $M_{\text{Pl}} = 1.22 \times 10^{19} \text{GeV}$ is the Planck mass, g_* the number of relativistic degrees of freedom at the freeze-out temperature T_f , and $x_f = m_0/T_f$ which, for m_0 in the range $1 - 20 \text{GeV}$, is in the range $18.2 - 19.4$. The quantity $\langle v_{12} \sigma_{\text{ann}} \rangle$ is the thermally averaged annihilation cross section of S_0 into fermion pairs $f\bar{f}$ for $m_f < m_0/2$, and into $S_1 S_1$ for $m_1 < m_0/2$. The annihilation cross-section into fermions proceeds via s-channel exchange of h and S_1 and is given by:

$$v_{12}\sigma_{S_0 S_0 \rightarrow f \bar{f}} = \frac{\sqrt{(m_0^2 - m_f^2)^3}}{4\pi m_0^3} \Theta(m_0 - m_f) \left[\frac{(\lambda_0^{(3)} \lambda_{hf})^2}{(4m_0^2 - m_h^2)^2 + \epsilon_h^2} + \frac{(\eta_{01}^{(3)} \lambda_{1f})^2}{(4m_0^2 - m_1^2)^2 + \epsilon_1^2} \right. \\ \left. + \frac{2\lambda_0^{(3)} \eta_{01}^{(3)} \lambda_{hf} \lambda_{1f} (4m_0^2 - m_h^2) (4m_0^2 - m_1^2)}{[(4m_0^2 - m_h^2)^2 + \epsilon_h^2][(4m_0^2 - m_1^2)^2 + \epsilon_1^2]} \right], \quad (15)$$

and the annihilation into S_1 pairs given by:

$$v_{12}\sigma_{S_0 S_0 \rightarrow S_1 S_1} = \frac{\sqrt{m_0^2 - m_1^2}}{64\pi m_0^3} \Theta(m_0 - m_1) \left[(\eta_{01}^{(4)})^2 + \frac{4\eta_{01}^{(4)} (\eta_{01}^{(3)})^2}{m_1^2 - 2m_0^2} + \frac{2\eta_{01}^{(4)} \eta_{01}^{(3)} \eta_1^{(3)}}{4m_0^2 - m_1^2} \right. \\ + \frac{2\eta_{01}^{(4)} \lambda_0^{(3)} \lambda_2^{(3)} (4m_0^2 - m_h^2)}{(4m_0^2 - m_h^2)^2 + \epsilon_h^2} + \frac{4(\eta_{01}^{(3)})^4}{(m_1^2 - 2m_0^2)^2} + \frac{4(\eta_{01}^{(3)})^3 \eta_1^{(3)}}{(4m_0^2 - m_1^2)(m_1^2 - 2m_0^2)} \\ + \frac{4(\eta_{01}^{(3)})^2 \lambda_0^{(3)} \lambda_2^{(3)} (4m_0^2 - m_h^2)}{[(4m_0^2 - m_h^2)^2 + \epsilon_h^2](m_1^2 - 2m_0^2)} + \frac{(\eta_{01}^{(3)})^2 (\eta_1^{(3)})^2}{(4m_0^2 - m_1^2)^2} \\ \left. + \frac{(\lambda_0^{(3)})^2 (\lambda_2^{(3)})^2}{(4m_0^2 - m_h^2)^2 + \epsilon_h^2} + \frac{2\eta_{01}^{(3)} \eta_1^{(3)} \lambda_0^{(3)} \lambda_2^{(3)} (4m_0^2 - m_h^2)}{[(4m_0^2 - m_h^2)^2 + \epsilon_h^2](4m_0^2 - m_1^2)} \right]. \quad (16)$$

Solving (14) with the current value for the dark matter relic density $\Omega_D \bar{h}^2 = 0.1123 \pm 0.0035$ [22] translates into a relation between the parameters of a given theory entering the calculated expression of $\langle v_{12}\sigma_{\text{ann}} \rangle$, hence imposing a constraint on these parameters which will limit the intervals of possible dark matter masses. This constraint is exploited to examine aspects of the theory like perturbativity, while at the same time reducing the number of parameters by one.

Indeed, the model starts with eight parameters. The spontaneous breaking of the electroweak and \mathbb{Z}_2 symmetries introduces the two vacuum expectation values v and v_1 respectively, which means we are left with six. Four of the parameters are the three physical masses m_0 (dark-matter singlet S_0), m_1 (the second singlet S_1) and m_h (Higgs h), plus the mixing angle θ between h and S_1 . We will fix the Higgs mass to $m_h = 125\text{GeV}$ [23, 24], except in the section discussing Higgs decays where we let m_h vary in the interval $100\text{GeV} - 200\text{GeV}$. We will take both m_0 and m_1 in the interval $0.1\text{GeV} - 10\text{GeV}$. For the purpose of our discussions, it is sufficient to let θ vary in the interval $1^\circ - 40^\circ$. The last parameters are the two physical mutual coupling constants $\lambda_0^{(4)}$ (dark matter – Higgs) and $\eta_{01}^{(4)}$ (dark matter – S_1 particle). But $\eta_{01}^{(4)}$ is not free as it is the smallest real and positive solution to the dark-matter relic density constraint (14), which will be implemented systematically throughout [17]. Thus we are left with four parameters, namely, m_0 , m_1 , θ and $\lambda_0^{(4)}$. To ensure applicability of perturbation

theory, the requirement $\eta_{01}^{(4)} < 1$ will also be imposed throughout, as well as a choice of rather small values for $\lambda_0^{(4)}$.

Studying the effects of the relic-density constraint for large ranges of the parameters through the behavior of the physical mutual coupling constant $\eta_{01}^{(4)}$ between S_0 and S_1 as a function of the DM mass m_0 shows that, apart from forbidden regions and others where perturbativity is lost, viable solutions in the small-moderate mass ranges of the DM sector exist for most values of the parameters [17]. Forbidden regions are found for most of the ranges of the parameters whereas perturbativity is lost mainly for larger values of m_1 .

2.2. Direct detection

On the other hand, experiments like CDMS II [15], XENON 10/100 [14, 25], DAMA/LIBRA [26] and CoGeNT [3] search directly for a dark matter signal, which would typically come from the elastic scattering of a dark matter WIMP off a non-relativistic nucleon target. However, throughout the years, such experiments have not yet detected an unambiguous signal, but rather yielded increasingly stringent exclusion bounds on the dark matter – nucleon elastic-scattering total cross-section σ_{det} in terms of the DM mass m_0 . Any viable theoretical dark-matter model has to satisfy these bounds. In the 2SSM, σ_{det} is found to be given by the relation [17]:

$$\sigma_{\text{det}} \equiv \sigma_{S_0 N \rightarrow S_0 N} = \frac{m_N^2 \left(m_N - \frac{7}{9}m_B\right)^2}{4\pi (m_N + m_0)^2 v^2} \left[\frac{\lambda_0^{(3)} \cos \theta}{m_h^2} - \frac{\eta_{01}^{(3)} \sin \theta}{m_1^2} \right]^2, \quad (17)$$

in which m_N is the nucleon mass and m_B the baryon mass in the chiral limit [13, 27, 28]. This relation was compared against the experimental bounds from CDMSII and XENON100. We found that strong constraints were imposed on m_0 in the range between 10 to 20 GeV. We found also that for small values of m_1 , very light dark matter is viable, with m_0 as small as 1 GeV.

3. Upsilon decays

We now further the analysis of the two-singlet model and start by looking at the constraints on the parameter space of the model coming from the decay of the meson Y in the state nS ($n = 1, 3$) into one photon γ and one particle S_1 . For $m_1 \lesssim 8\text{ GeV}$, the branching ratio for this process is given by the relation:

$$\text{Br}(Y_{nS} \rightarrow \gamma + S_1) = \frac{G_F m_b^2 \sin^2 \theta}{\sqrt{2}\pi\alpha} x_n \left(1 - \frac{4\alpha_s}{3\pi} f(x_n)\right) \text{Br}^{(\mu)} \Theta(m_{Y_{nS}} - m_1). \quad (18)$$

In this expression, $x_n \equiv \left(1 - m_1^2/m_{Y_{nS}}^2\right)$ with $m_{Y_{1(3)S}} = 9.46(10.355)\text{ GeV}$ the mass of $Y_{1(3)S}$, the branching ratio $\text{Br}^{(\mu)} \equiv \text{Br}(Y_{1(3)S} \rightarrow \mu^+ \mu^-) = 2.48(2.18) \times 10^{-2}$ [29], α is the QED coupling constant, $\alpha_s = 0.184$ the QCD coupling constant at the scale $m_{Y_{nS}}$, the quantity G_F

is the Fermi coupling constant and m_b the b quark mass [22]. The function $f(x)$ incorporates the effect of QCD radiative corrections given in [30].

But the above expression is not sufficient because a rough estimate of the lifetime of S_1 indicates that this latter is likely to decay inside a typical particle detector, which means we ought to take into account its most dominant decay products. We first have a process by which S_1 decays into a pair of pions, with a decay rate given by:

$$\begin{aligned} \Gamma(S_1 \rightarrow \pi\pi) \simeq & \frac{G_F m_1}{4\sqrt{2}\pi} \sin^2 \theta \left[\frac{m_1^2}{27} \left(1 + \frac{11m_\pi^2}{2m_1^2} \right)^2 \right. \\ & \times \left(1 - \frac{4m_\pi^2}{m_1^2} \right)^{\frac{1}{2}} \Theta[(m_1 - 2m_\pi)(2m_K - m_1)] \\ & \left. + 3(M_u^2 + M_d^2) \left(1 - \frac{4m_\pi^2}{m_1^2} \right)^{\frac{3}{2}} \Theta(m_1 - 2m_K) \right]. \end{aligned} \quad (19)$$

In the above decay rate, $m_{\pi(K)}$ is the pion (kaon) mass. Also, chiral perturbation theory is used below the kaon pair production threshold [31, 32], and the spectator quark model above up to roughly 3GeV, with the dressed u and d quark masses $M_u = M_d \simeq 0.05\text{GeV}$. Note that this rate includes all pions, charged and neutral. Above the $2m_K$ threshold, both pairs of kaons and η particles are produced. The decay rate for K production is:

$$\Gamma(S_1 \rightarrow KK) \simeq \frac{9}{13} \frac{3G_F M_s^2 m_1}{4\sqrt{2}\pi} \sin^2 \theta \left(1 - \frac{4m_K^2}{m_1^2} \right)^{\frac{3}{2}} \Theta(m_1 - 2m_K). \quad (20)$$

In the above rate, $M_s \simeq 0.45\text{GeV}$ is the s quark-mass in the spectator quark model [33, 34]. For η production, replace m_K by m_η and $\frac{9}{13}$ by $\frac{4}{13}$.

The particle S_1 can also decay into c and b quarks (mainly c). Including the radiative QCD corrections, the corresponding decay rates are given by:

$$\Gamma(S_1 \rightarrow q\bar{q}) \simeq \frac{3G_F \bar{m}_q^2 m_1}{4\sqrt{2}\pi} \sin^2 \theta \left(1 - \frac{4\bar{m}_q^2}{m_1^2} \right)^{\frac{3}{2}} \left(1 + 5.67 \frac{\bar{\alpha}_s}{\pi} \right) \Theta(m_1 - 2\bar{m}_q). \quad (21)$$

The dressed quark mass $\bar{m}_q \equiv m_q(m_1)$ and the running strong coupling constant $\bar{\alpha}_s \equiv \alpha_s(m_1)$ are defined at the energy scale m_1 [35]. Gluons can also be produced, with a corresponding decay rate given by the relation:

$$\Gamma(S_1 \rightarrow gg) \simeq \frac{G_F m_1^3 \sin^2 \theta}{12\sqrt{2}\pi} \left(\frac{\alpha'_s}{\pi} \right)^2 \left[6 - 2 \left(1 - \frac{4m_\pi^2}{m_1^2} \right)^{\frac{3}{2}} - \left(1 - \frac{4m_K^2}{m_1^2} \right)^{\frac{3}{2}} \right] \Theta(m_1 - 2m_K). \quad (22)$$

Here, $\alpha'_s = 0.47$ is the QCD coupling constant at the spectator-quark-model scale, between roughly 1GeV and 3GeV.

We then have the decay of S_1 into leptons, the corresponding rate given by:

$$\Gamma(S_1 \rightarrow \ell^+ \ell^-) = \frac{G_F m_\ell^2 m_1}{4\sqrt{2}\pi} \sin^2 \theta \left(1 - \frac{4m_\ell^2}{m_1^2}\right)^{\frac{3}{2}} \Theta(m_1 - 2m_\ell), \quad (23)$$

where m_ℓ is the lepton mass. Finally, S_1 can decay into a pair of dark matter particles, with a decay rate:

$$\Gamma(S_1 \rightarrow S_0 S_0) = \frac{(\eta_{01}^{(3)})^2}{32\pi m_1} \sqrt{1 - \frac{4m_0^2}{m_1^2}} \Theta(m_1 - 2m_0). \quad (24)$$

The branching ratio for Y_{nS} decaying via S_1 into a photon plus X , where X represents any kinematically allowed final state, will be:

$$\text{Br}(Y_{nS} \rightarrow \gamma + X) = \text{Br}(Y_{nS} \rightarrow \gamma + S_1) \times \text{Br}(S_1 \rightarrow X). \quad (25)$$

In particular, $X \equiv S_0 S_0$ corresponds to a decay into invisible particles.

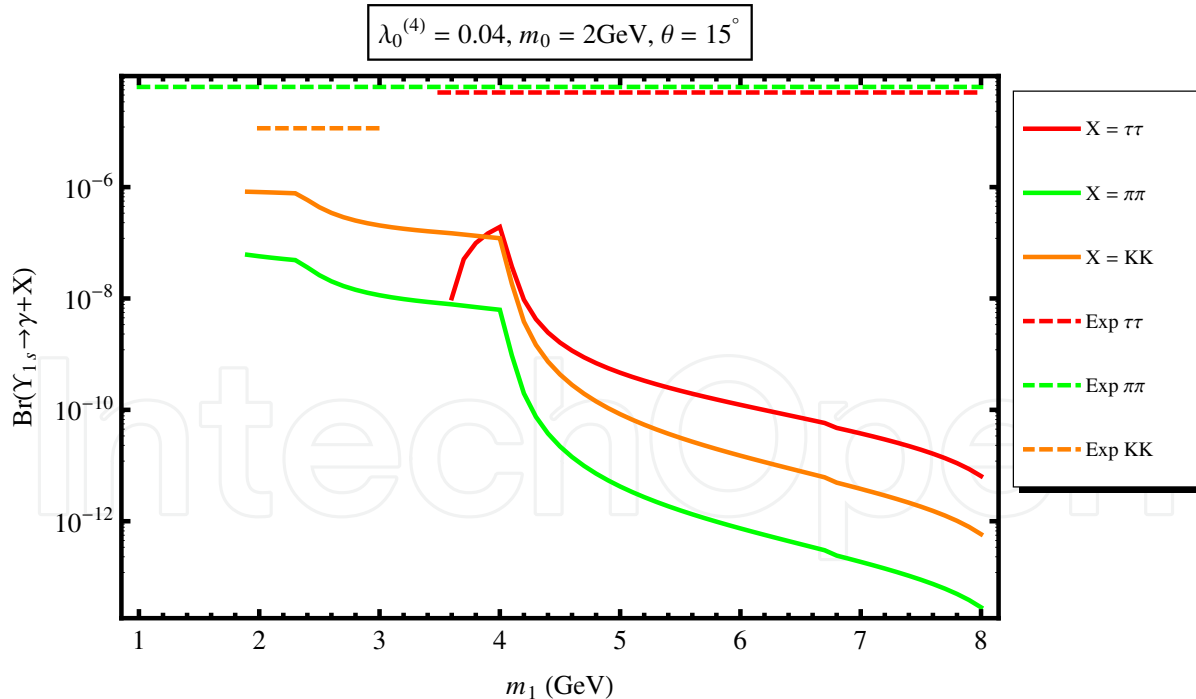


Figure 1. Typical branching ratios of Y_{1S} decaying into τ 's, charged pions and charged kaons as functions of m_1 . The corresponding experimental upper bounds are shown.

The best available experimental upper bounds on $1S$ -state branching ratios are: (i) $\text{Br}(Y_{1S} \rightarrow \gamma + \tau\tau) < 5 \times 10^{-5}$ for $3.5\text{GeV} < m_1 < 9.2\text{GeV}$ [36]; (ii) $\text{Br}(Y_{1S} \rightarrow \gamma + \pi^+ \pi^-) <$

6.3×10^{-5} for $1\text{GeV} < m_1$ [37]; (iii) $\text{Br}(Y_{1S} \rightarrow \gamma + K^+ K^-) < 1.14 \times 10^{-5}$ for $2\text{GeV} < m_1 < 3\text{GeV}$ [38]. Figure 1 displays the corresponding branching ratios of Y_{1S} decays via S_1 as functions of m_1 , together with these upper bounds. Also, the best available experimental upper bounds on Y_{3S} branching ratios are: (i) $\text{Br}(Y_{3S} \rightarrow \gamma + \mu\mu) < 3 \times 10^{-6}$ for $1\text{GeV} < m_1 < 10\text{GeV}$; (ii) $\text{Br}(Y_{3S} \rightarrow \gamma + \text{Invisible}) < 3 \times 10^{-6}$ for $1\text{GeV} < m_1 < 7.8\text{GeV}$ [39]. Typical corresponding branching ratios are shown in figure 2.

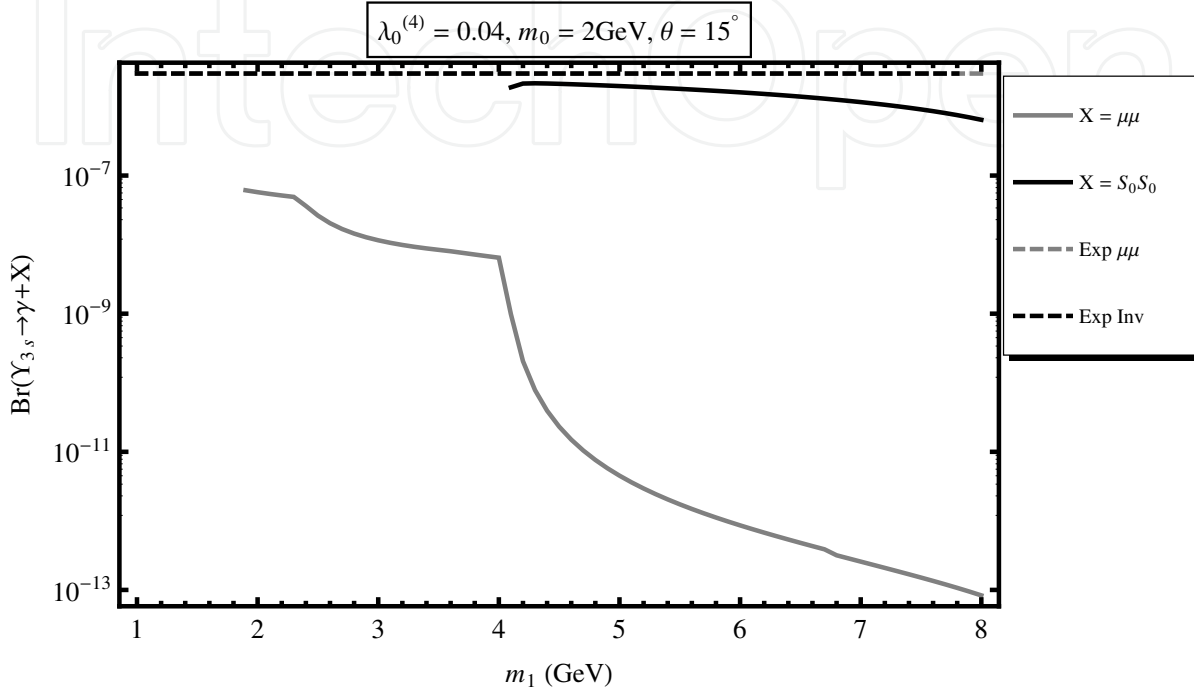


Figure 2. Typical branching ratios of Y_{3S} decaying into muons and dark matter as functions of m_1 . The corresponding experimental upper bounds are shown.

When scanning the parameter space, we see that the Higgs-dark-matter coupling constant $\lambda_0^{(4)}$ and the dark-matter mass m_0 have little effect on the shapes of the branching ratios, apart from excluding, via the relic density and perturbativity constraints, regions of applicability of the model. This shows in figures 1 and 2 where the region $m_1 \lesssim 1.9\text{GeV}$ is excluded. Also, the onset of the $S_0 S_0$ channel for $m_1 \geq 2m_0$ abates sharply the other channels as this one becomes dominant by far. The effect of the mixing angle θ is to enhance all branching ratios as it increases, due to the factor $\sin^2 \theta$. Furthermore, we notice that the dark matter decay channel reaches the invisible upper bound already for $\theta \simeq 15^\circ$, for fairly small m_0 , say 0.5GeV , whereas the other channels find it hard to get to their respective experimental upper bounds, even for large values of θ .

4. B meson decays

Next we look at the flavor changing process in which the meson B^+ decays into a K^+ plus invisible. The corresponding Standard-Model mode is a decay into K^+ and a pair of neutrinos, with a branching ratio $\text{Br}^{\text{SM}}(B^+ \rightarrow K^+ + \nu\bar{\nu}) \simeq 4.7 \times 10^{-6}$ [40]. The experimental upper bound is $\text{Br}^{\text{Exp}}(B^+ \rightarrow K^+ + \text{Inv}) \simeq 14 \times 10^{-6}$ [41]. Here too, the most prominent B

invisible decay is into $S_0 S_0$ via S_1 . The process $B^+ \rightarrow K^+ + S_1$ has the following branching ratio:

$$\text{Br}(B^+ \rightarrow K^+ + S_1) = \frac{9\sqrt{2}\tau_B G_F^3 m_t^4 m_b^2 m_+^2 m_-^2}{1024\pi^5 m_B^3 (m_b - m_s)^2} |V_{tb} V_{ts}^*|^2 f_0^2(m_1^2) \times \sqrt{(m_+^2 - m_1^2)(m_-^2 - m_1^2)} \sin^2 \theta \Theta(m_- - m_1). \quad (26)$$

In the above relation, $m_{\pm} = m_B \pm m_K$ where m_B is the B^+ mass, τ_B its lifetime, and V_{tb} and V_{ts} are flavor changing CKM coefficients. The function $f_0(s)$ is given by the relation:

$$f_0(s) = 0.33 \exp \left[\frac{0.63s}{m_B^2} - \frac{0.095s^2}{m_B^4} + \frac{0.591s^3}{m_B^6} \right]. \quad (27)$$

The different S_1 decay modes are given in (19) - (24) above. The branching ratio of B^+ decaying into $K^+ + S_0 S_0$ via the production and propagation of an intermediary S_1 will be:

$$\text{Br}^{(S_1)}(B^+ \rightarrow K^+ + S_0 S_0) = \text{Br}(B^+ \rightarrow K^+ + S_1) \times \text{Br}(S_1 \rightarrow S_0 S_0). \quad (28)$$

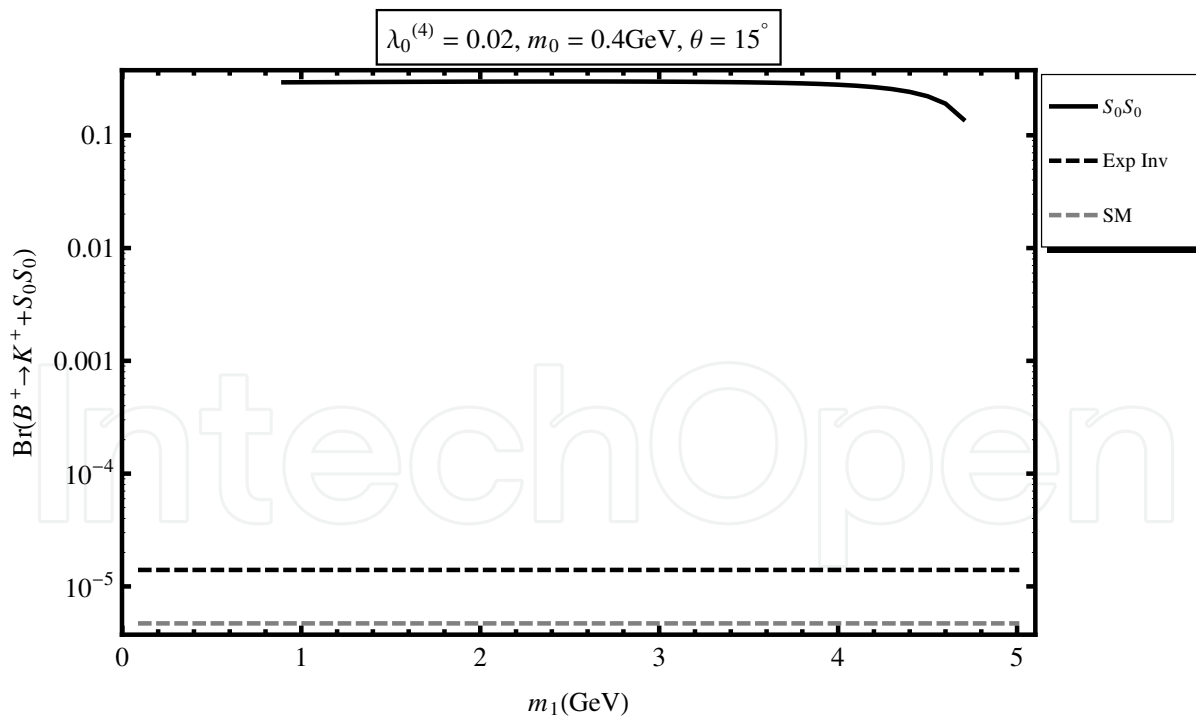


Figure 3. Typical branching ratio of B^+ decaying into dark matter via S_1 as a function of m_1 . The SM and experimental bounds are shown.

Figure 3 displays a typical behavior of $\text{Br}^{(S_1)}(B^+ \rightarrow K^+ + S_0 S_0)$ as a function of m_1 . As we see, the branching ratio is well above the experimental upper bound, and a mixing angle θ

as small as 1° will not help with this, no matter what the values for $\lambda_0^{(4)}$ and m_0 are. So, we conclude that for $m_1 \lesssim 4.8\text{GeV}$, this process excludes the two-singlet model for $m_0 < m_1/2$. For $m_1 \gtrsim 4.8\text{GeV}$ or $m_0 \geq m_1/2$, the decay does not occur, so no constraints on the model from this process.

Another process involving B mesons is the decay of B_s into predominately a pair of muons. The Standard Model branching ratio for this process is $\text{Br}^{\text{SM}}(B_s \rightarrow \mu^+\mu^-) = (3.2 \pm 0.2) \times 10^{-9}$ [42], and the experimental upper bound is $\text{Br}^{\text{Exp}}(B_s \rightarrow \mu^+\mu^-) < 1.08 \times 10^{-8}$ [43]. In the present model, two additional decay diagrams occur, both via intermediary S_1 , yielding together the branching ratio:

$$\text{Br}^{(S_1)}(B_s \rightarrow \mu^+\mu^-) = \frac{9\tau_{B_s} G_F^4 f_{B_s}^2 m_{B_s}^5}{2048\pi^5} m_\mu^2 m_t^4 |V_{tb} V_{ts}^*|^2 \frac{(1 - 4m_\mu^2/m_{B_s}^2)^{3/2}}{(m_{B_s}^2 - m_1^2)^2 + m_1^2 \Gamma_1^2} \sin^4 \theta. \quad (29)$$

In this relation, τ_{B_s} is the B_s life-time, $m_{B_s} = 5.37\text{GeV}$ its mass, and f_{B_s} a form factor that we take equal to 0.21GeV . The quantity Γ_1 is the total width of the particle S_1 [17].

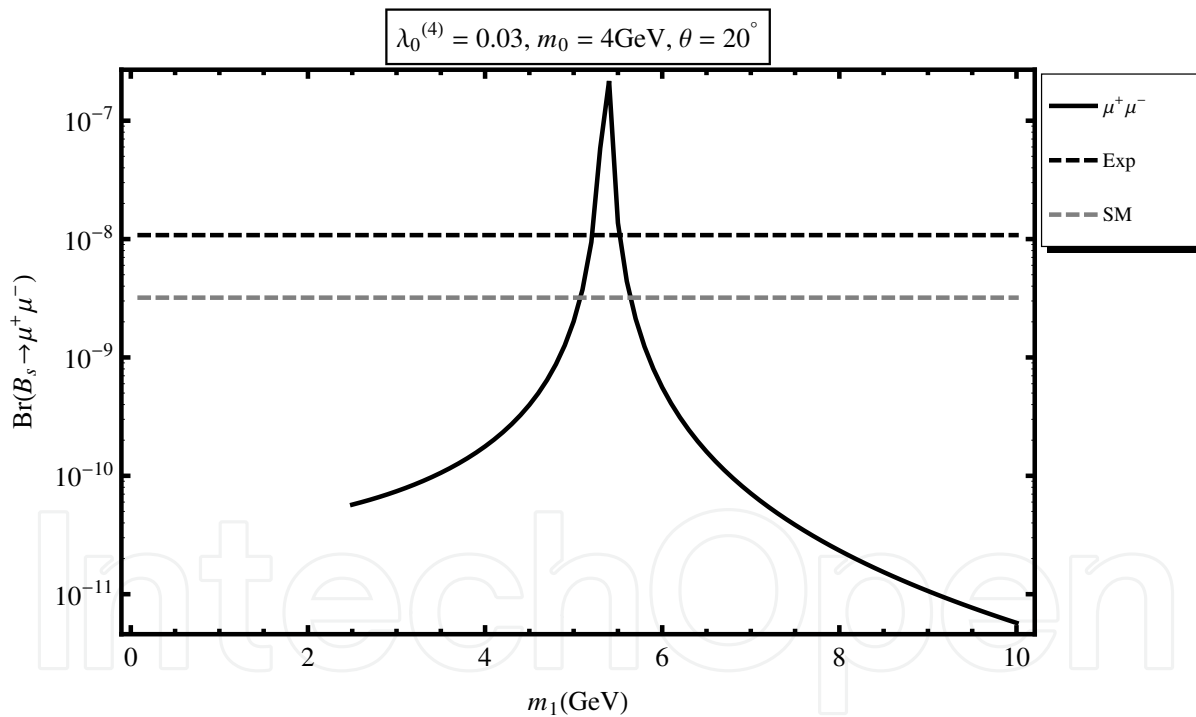


Figure 4. Typical behavior of $\text{Br}^{(S_1)}(B_s \rightarrow \mu^+\mu^-)$ as a function of m_1 , together with the SM and experimental bounds.

A typical behavior of $\text{Br}^{(S_1)}(B_s \rightarrow \mu^+\mu^-)$ as a function of m_1 is displayed in figure 4. The peak is at m_{B_s} . All three parameters $\lambda_0^{(4)}$, m_0 and θ combine in the relic density constraint to exclude few regions of applicability of the model. For example, for the values of figure 4, the region $m_1 < 2.25\text{GeV}$ is excluded. However, a systematic scan of the parameter space shows that outside the relic density constraint, $\lambda_0^{(4)}$ has no significant direct effect on the shape of $\text{Br}^{(S_1)}(B_s \rightarrow \mu^+\mu^-)$. As m_0 increases, it sharpens the peak of the curve while pushing it up.

This works until about 2.7GeV, beyond which m_0 ceases to have any significant direct effect. Increasing θ enhances the values of the branching ratio without affecting the width. Also, for all the range of m_1 , all of $\text{Br}^{(S_1)} + \text{Br}^{\text{SM}}$ stays below Br^{Exp} as long as $\theta < 10^\circ$. As θ increases beyond this value, the peak region pushes up increasingly above Br^{Exp} , like in figure 4, and hence gets excluded, but all the rest is allowed.

5. Higgs decays

We finally examine the implications of the model on the Higgs different decay modes. In this section, we allow the Higgs mass m_h to vary in the interval 100GeV – 200GeV. First, h can decay into a pair of leptons ℓ , predominantly τ 's. The corresponding decay rate $\Gamma(h \rightarrow \ell^+ \ell^-)$ is given by the relation (23) where we replace m_1 by m_h and $\sin \theta$ by $\cos \theta$. It can also decay into a pair of quarks q , mainly into b 's and, to a lesser degree, into c 's. Here too the decay rate $\Gamma(h \rightarrow q \bar{q})$ is given in (21) with similar replacements. Then the Higgs can decay into a pair of gluons. The corresponding decay rate that includes the next-to-next-to-leading QCD radiative corrections is given by:

$$\Gamma(h \rightarrow gg) = \frac{G_F m_h^3}{4\sqrt{2}\pi} \left| \sum_q \frac{m_q^2}{m_h^2} \int_0^1 dx \int_0^{1-x} dy \frac{1-4xy}{\frac{m_q^2}{m_h^2} - xy} \right|^2 \times \left(\frac{\bar{\alpha}_s}{\pi} \right)^2 \left[1 + \frac{215}{12} \frac{\bar{\alpha}_s}{\pi} + \frac{\bar{\alpha}_s^2}{\pi^2} \left(156.8 - 5.7 \log \frac{m_t^2}{m_h^2} \right) \right] \cos^2 \theta, \quad (30)$$

where the sum is over all quark flavors q . A systematic study of the double integral above shows that, with m_h in the range 100GeV – 200GeV, the t quark dominates in the sum over q , but with non-negligible contributions from the c and b quarks.

For m_h smaller than the W or Z pair-production thresholds, the Higgs can decay into a pair of one real and one virtual gauge bosons, with rates given by:

$$\Gamma(h \rightarrow VV^*) = \frac{3G_F^2 m_V^4 m_h}{16\pi^3} \cos^2 \theta A_V R \left(\frac{m_V^2}{m_h^2} \right) \Theta[(m_h - m_V)(2m_V - m_h)]. \quad (31)$$

In this expression, m_V is the mass of the gauge boson V , the factor $A_V = 1$ for W and $\left(\frac{7}{12} - \frac{10}{9} \sin^2 \theta_w + \frac{40}{9} \sin^4 \theta_w \right)$ for Z with θ_w the Weinberg angle, and we have the definition:

$$R(x) = \frac{3(1-8x+20x^2)}{\sqrt{4x-1}} \arccos \left(\frac{3x-1}{2x^{3/2}} \right) - \frac{1-x}{2x} \left(2-13x+47x^2 \right) - \frac{3}{2} \left(1-6x+4x^2 \right) \log x. \quad (32)$$

For a heavier Higgs particle, the decay rates into a V pair is given by:

$$\Gamma(h \rightarrow VV) = \frac{G_F m_V^4 \cos^2 \theta}{\sqrt{2} \pi m_h} B_V \left(1 - \frac{4m_V^2}{m_h^2}\right)^{\frac{1}{2}} \left[1 + \frac{(m_h^2 - 2m_V^2)^2}{8m_V^4}\right] \Theta(m_h - 2m_V), \quad (33)$$

with $B_V = 1$ for W and $\frac{1}{2}$ for Z .

While all these decay modes are already present within the Standard Model, the two-singlet extension introduces two additional (invisible) modes, namely a decay into a pair of S_0 's and a pair of S_1 's. The corresponding decay rates are:

$$\Gamma(h \rightarrow S_i S_i) = \frac{\lambda_i^2}{32 \pi m_h} \left(1 - \frac{4m_i^2}{m_h^2}\right)^{\frac{1}{2}} \Theta(m_h - 2m_i), \quad (34)$$

where $\lambda_i = \lambda_{0(2)}^{(3)}$ for $S_{0(1)}$ given in (9). The total decay rate $\Gamma(h)$ of the Higgs particle is the sum of these partial rates. The branching ratio corresponding to a particular decay will be $\text{Br}(h \rightarrow X) = \Gamma(h \rightarrow X) / \Gamma(h)$.

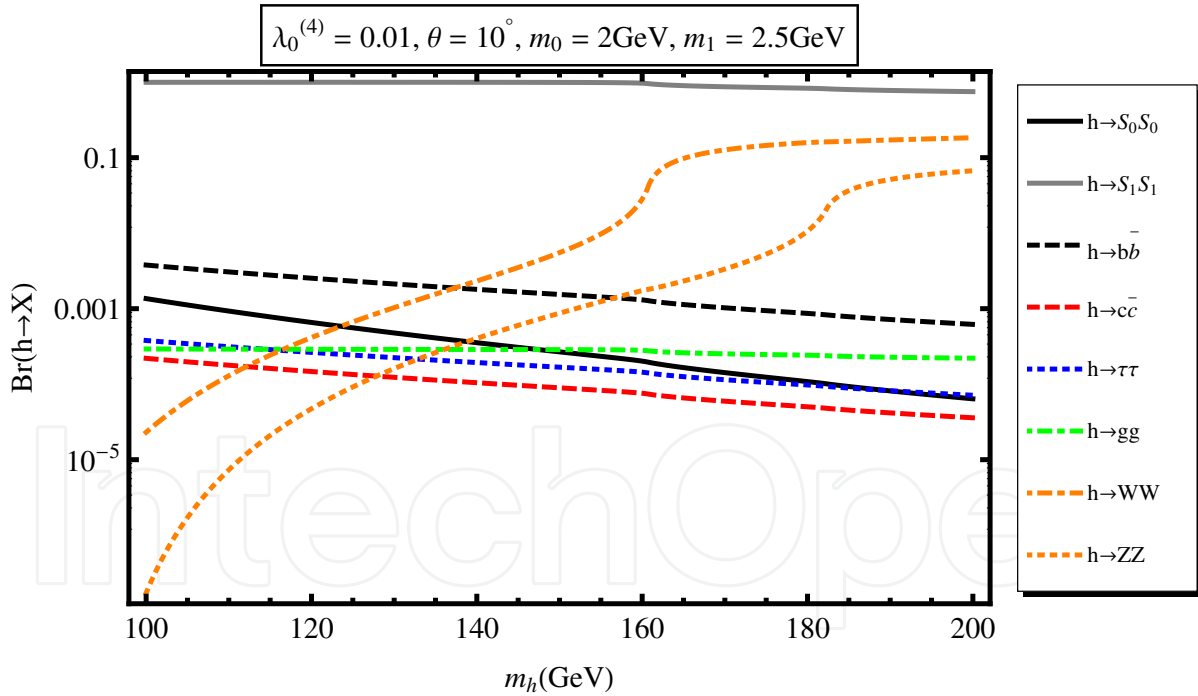


Figure 5. Branching ratios for Higgs decays. Very small dark-matter Higgs coupling.

Typical behaviors of the most prominent branching ratios are displayed in figure 5. A systematic study shows that for all ranges of the parameters, the Higgs decays dominantly into invisible. The production of fermions and gluons is comparatively marginal, whereas that of W and Z pairs takes relative importance towards and above the corresponding thresholds, and more significantly at larger values of the mixing angle θ .

However, the decay distribution between S_0 and S_1 is not even. The most dramatic effect comes from the coupling constant $\lambda_0^{(4)}$. When it is very small, the dominant production is that of a pair of S_1 . This is exhibited in figure 5 for which $\lambda_0^{(4)} = 0.01$. As it increases, there is a gradual shift towards a more dominating dark-matter pair production, a shift competed against by the increase in θ . Figure 6 displays the branching ratios for $\lambda_0^{(4)} = 0.1$ and figure 7 for the larger value $\lambda_0^{(4)} = 0.7$. In general, increasing θ smoothens the crossings of the WW and ZZ thresholds, and lowers the production of everything except that of a pair of S_1 , which is instead increased.

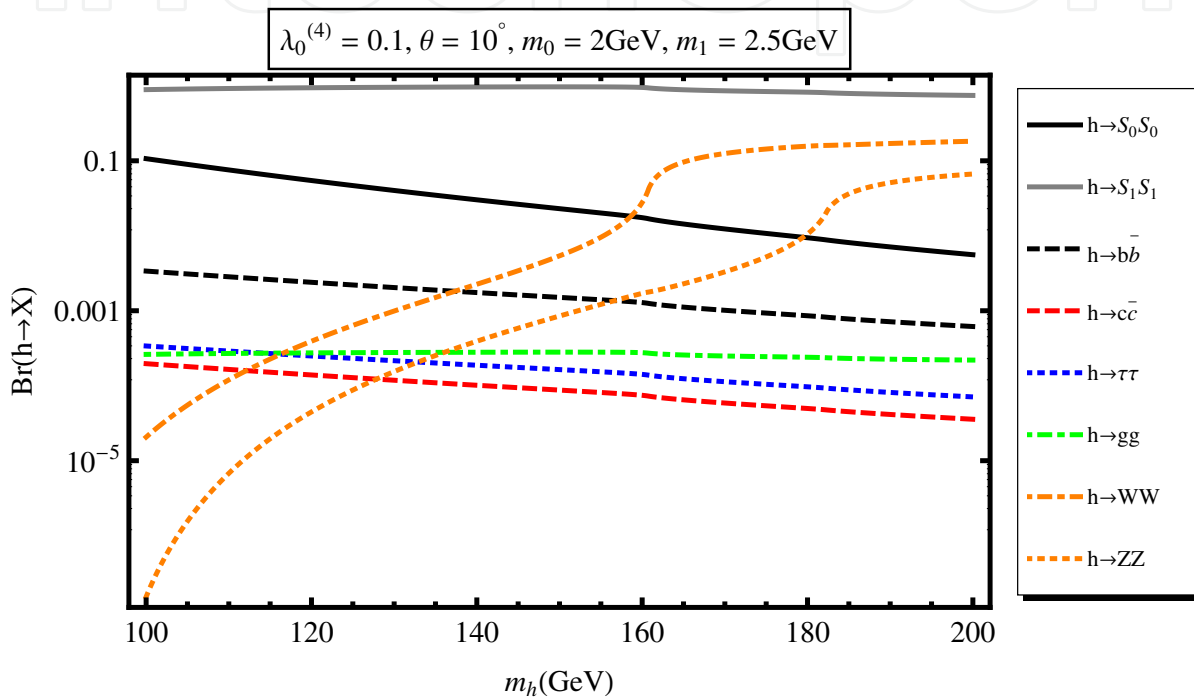


Figure 6. Branching ratios for Higgs decays. Small dark-matter Higgs coupling.

Like in the Standard Model, the production of a pair of b quarks dominates over the production of the other fermions, and all fermions are not favored by increasing $\lambda_0^{(4)}$. Changes in m_0 and m_1 have very little direct effects on all the branching ratios except that of $S_0 S_0$ production where, at small θ , increasing m_1 (m_0) increases (decreases) the branching ratio, with reversed effects at larger θ . Note though that these masses have indirect impact through the relic density constraint by excluding certain regions [17].

6. Concluding remarks

Understanding light dark matter is one of the challenges facing popular extensions of the Standard Model. In this chapter, we have furthered the study of a two-singlet extension of the SM we proposed as a model for light dark matter by exploring some of its phenomenological aspects. We have looked into the rare decays of Y and B mesons and studied the implications of the model on the decay channels of the Higgs particle.

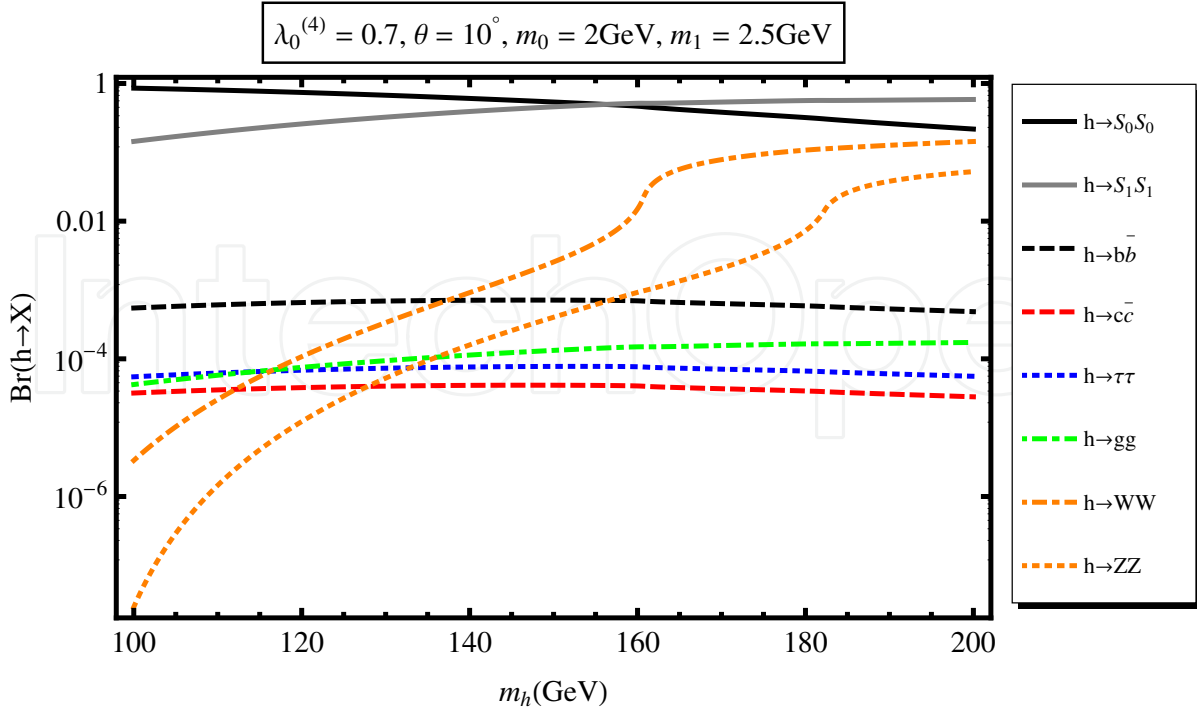


Figure 7. Branching ratios for Higgs decays. Larger dark-matter Higgs coupling.

In brief, for both Y and B decays, the Higgs-DM coupling constant $\lambda_0^{(4)}$ and the DM mass m_0 have little effect on the shapes of the branching ratios, apart from combining with the other two parameters in the relic-density and perturbativity constraints to exclude regions of applicability of the model. Also, the effect of increasing the $h - S_1$ mixing angle θ is to enhance all branching ratios. For Y decays, the DM channel dominates over the other decay modes in regions where kinematically allowed. It reaches the experimental invisible upper bound for already fairly small values of θ and m_0 . From B^+ decays, we learn that our model is excluded for $m_1 < 4.8\text{GeV}$ ($= m_B - m_K$) and $m_0 < m_1/2$. From B_s decay into muons, we learn that for the model to contribute a distinct signal to this process, it is best to restrict $4\text{GeV} \lesssim m_1 \lesssim 6.5\text{GeV}$ with no additional constraint on m_0 [20]. Also, in general, keeping $\lambda_0^{(4)} \lesssim 0.1$ to avoid systematic exclusion from direct detection for all these processes is safe.

Before closing the chapter, it is useful to comment briefly on how light dark matter in our model affects Higgs searches. Since $m_h \gg 2m_0$, the process $h \rightarrow S_0 S_0$ is kinematically allowed and, for a large range of the parameter space, the ratio

$$\mathcal{R}_{\text{decay}}^{(b)} = \frac{\text{Br}(h \rightarrow S_0 S_0)}{\text{Br}(h \rightarrow b\bar{b})} \quad (35)$$

can be larger than one for $m_h < 120\text{GeV}$ as can be seen in figure 6. In this situation, the LEP bound on the Higgs mass can be weaker. Also, in our model, the Higgs production at LEP via Higgstrahlung can be smaller than the one in the Standard Model, and so the Higgs can be as light as 100GeV . Such a light Higgs would be in good agreement with the electroweak precision tests. As to the Higgs searches at the LHC, the ATLAS and CMS collaborations have reported the exclusion of a Higgs mass in the interval $145 - 460\text{ GeV}$ [23, 24], which

seems to suggest that we should have limited our analysis of the Higgs branching ratios to $m_h < 145\text{GeV}$. However, it is important to note that these experimental constraints apply to the SM Higgs and can not therefore be used as such if the Higgs interactions are modified. In our model, the mixing of h with S_1 will result in a reduction of the statistical significance of the Higgs discovery at the LHC. Indeed, the relevant quantity that allows one to use the experimental limits on Higgs searches to derive constraints on the parameters of the model is the ratio:

$$\mathcal{R}_{X_{\text{SM}}} \equiv \frac{\sigma(gg \rightarrow h) \text{Br}(h \rightarrow X_{\text{SM}})}{\sigma^{(\text{SM})}(gg \rightarrow h) \text{Br}^{\text{SM}}(h \rightarrow X_{\text{SM}})} = \frac{\cos^4 \theta}{\cos^2 \theta + \Gamma(h \rightarrow X_{\text{inv}}) / \Gamma_h^{\text{SM}}}. \quad (36)$$

In this expression, X_{SM} corresponds to all the Standard Model particles, $X_{\text{inv}} = S_0 S_0$ and $S_1 S_1$, σ is a cross-section, $\text{Br}^{\text{SM}}(h \rightarrow X)$ the branching fraction of the SM Higgs decaying into any kinematically allowed mode X , and Γ_h^{SM} the total Higgs decay rate in the Standard Model. To open up the region $m_h > 140\text{GeV}$ requires the ratio $\mathcal{R}_{X_{\text{SM}}}$ to be smaller than 0.25 [23, 24], a constraint easily fulfilled in our model. By comparison, the minimal extensions of the Standard Model with just one singlet scalar or a Majorana fermion, even under a Z_2 symmetry, are highly constrained in this regard [44]. Finally, if the recent data from ATLAS and CMS turn out to be a signal for a SM-like Higgs with mass about 125GeV , then this will put a very strong constraint on the mixing angle θ . Indeed, only for $\theta \lesssim 0.5^\circ$ will the ratio $\Gamma(h \rightarrow b\bar{b}) / \Gamma(h \rightarrow \text{inv}) \gtrsim 1$. For larger values, the model is ruled out, independently of the dark matter mass, but as long as $m_1 \lesssim 50\text{GeV}$, which we are assuming in this work.

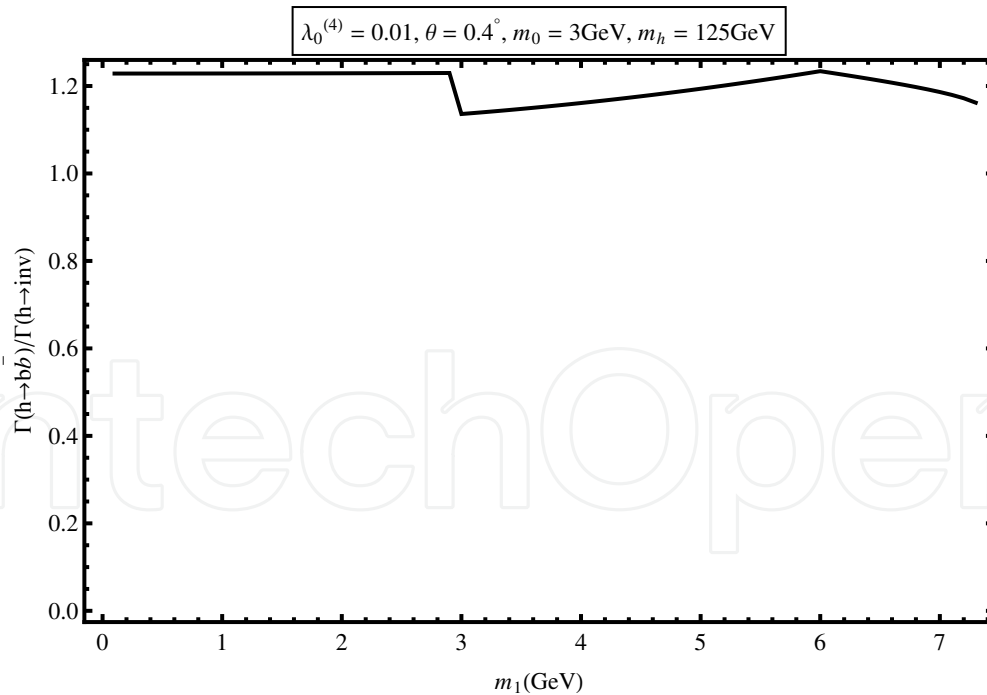


Figure 8. The ratio $\Gamma(h \rightarrow b\bar{b}) / \Gamma(h \rightarrow \text{inv})$ is larger than one for $\theta = 0.4^\circ$ and $m_h = 125\text{GeV}$.

Finally, it is important to find the bounds on the mass SM Higgs that can satisfy the triviality and perturbativity constraints on the coupling constants in the scalar sector of this model up to a scale higher than 1TeV . This requires studying the renormalization group equations of these coupling constants [45].

Author details

Abdessamad Abada^{1,2} and Salah Nasri²

* Address all correspondence to: a.abada@uaeu.ac.ae; snasri@uaeu.ac.ae

1 Laboratoire de Physique des Particules et Physique Statistique, Ecole Normale Supérieure, BP 92 Vieux Kouba, Alger, Algeria

2 Physics Department, United Arab Emirates University, POB, Al Ain, United Arab Emirates

References

- [1] Ellis, J., Hagelin, J.S., Nanopoulos, D.V., Olive, K.A., and Srednicki, M., Nucl. Phys. B238, 453 (1984).
- [2] Jungman, G., Kamionkowski, M., and Griest, K., Phys. Rept. 267, 195 (1996) (arXiv:hep-ph/9506380).
- [3] Aalseth, C.E. *et al.*, Phys. Rev. Lett. 107, 141301 (2011); Phys. Rev. Lett. 106, 131301 (2011).
- [4] Fornengo, N., Scopel, S., and Bottino, A., Phys. Rev. D 83, 015001 (2011); Niro, V., Bottino, A., Fornengo, N. and Scopel, S., Phys. Rev. D 80, 095019 (2009).
- [5] Cumberbatch, D.T., Lopez-Fogliani, D.E., Roszkowski, L., de Austri, R.R., and Tsai, Y.L., arXiv:1107.1604 [astro-ph.CO]; Vasquez, D.A., Belanger, G., Boehm, C., Pukhov, A., and Silk, J., Phys. Rev. D 82, 115027 (2010); Kuflik, E., Pierce, A., and Zurek, K.M., Phys. Rev. D 81, 111701 (2010); Feldman, D., Liu, Z., and Nath, P., Phys. Rev. D 81, 117701 (2010).
- [6] Gunion, J.F., Belikov, A.V., and Hooper, D., arXiv:1009.2555 [hep-ph]; Cumberbatch, D.T., Lopez-Fogliani, D.E., Roszkowski, L., de Austri, R.R., and Tsai, Y.L., arXiv:1107.1604 [astro-ph.CO].
- [7] Mambrini, Y., arXiv:1108.0671 [hep-ph]; Kajiyama, Y., Okada, H., and Toma, T., arXiv:1109.2722 [hep-ph]; Cline, J.M., and Frey, A.R., Phys. Rev. D 84, 075003 (2011); Kappl, R., Ratz, M., and Winkler, M.W., Phys. Lett. B 695, 169 (2011); Mambrini, Y., and Zaldivar, B., JCAP 1110, 023 (2011); Draper, P., Liu, T., Wagner, C.E.M., Wang, L.T.M., and Zhang, H., Phys. Rev. Lett. 106, 121805 (2011); Foot, R., Phys. Lett. B 703, 7 (2011); Gonderinger, M., Li, Y., Patel, H., and Ramsey-Musolf, M.J., JHEP 053, 1001 (2010); Andreas, S., Arina, C., Hambye, T., Ling, F.S., and Tytgat, M.H.G., Phys. Rev. D 82, 043522 (2010); Bae, K.J., Kim, H.D., and Shin, S., Phys. Rev. D 82, 115014 (2010); Farina, M., Pappadopulo, D., and Strumia, A., Phys. Lett. B 688, 329 (2010); Barger, V., Langacker, P., McCaskey, M., Ramsey-Musolf, M.J., and Shaughnessy, G., Phys. Rev. D 77, 035005 (2008).
- [8] Silveira, V., and Zee, A.; Phys. Lett. B161, 136 (1985).
- [9] McDonald, J., Phys. Rev. D 50, 3637 (1994).
- [10] Burgess, C., Pospelov, M., and ter Veldhuis, T.; Nucl. Phys. B619, 709 (2001).

- [11] Barger, V., Langacker, P., McCaskey, M., Ramsey-Musolf, M., and Shaughnessy, G.; Phys. Rev. D 77, 035005 (2008) (arXiv:0706.4311 [hep-ph]).
- [12] Gonderinger, M., Li, Y., Patel, H., and Ramsey-Musolf, M.; JHEP 053, 1001 (2010) (arXiv:0910.3167 [hep-ph]).
- [13] He, X., Li, T., Li, X., Tandean, J. and Tsai, H.; Phys. Rev. D 79, 023521 (2009) (arXiv:0811.0658 [hep-ph]).
- [14] Angle, J., *et al.* [XENON Collaboration], Phys. Rev. Lett. 100, 021303 (2008) (arXiv:0706.0039 [astro-ph]).
- [15] Ahmed, Z., *et al.* [CDMS Collaboration], Phys. Rev. Lett. 102, 011301 (2009) (arXiv:0802.3530 [astro-ph]); Ahmed, Z., *et al.* [CDMS Collaboration], Science 327, 1619 (2010) (arXiv:0912.3592 [astro-ph.CO]).
- [16] Arina, C. and Tytgat, M.; JCAP 1101, 011 (2011).
- [17] Abada, A., Ghaffor, D., and Nasri, S., Phys. Rev. D 83 095021 (2011) [arXiv:1101.0365[hep-ph]].
- [18] Ahriche, A. and Nasri, S., Phys. Rev. D 85, 093007 (2012) (arXiv:1201.4614 [hep-ph]).
- [19] Barger, V., Langacker, P., McCaskey, M., Ramsey-Musolf, M., and Shaughnessy, G., Phys. Rev. D 79, 015018 (2009) [arXiv:0811.0393 [hep-ph]].
- [20] Abada, A., and Nasri, S., Phys. Rev. D 85, 075009 (2012) (arXiv:1201.1413 [hep-ph]).
- [21] Kolb, E.W., and Turner, M.S., *'The Early Universe'*, Addison-Wesley, (1998).
- [22] Nakamura, K., *et al.* (Particle Data Group), JP G 37, 075021 (2010).
- [23] [ATLAS Collaboration], arXiv:1112.2577 [hep-ex]; Aad, G., *et al.* [ATLAS Collaboration], Eur. Phys. J. C 71, 1728 (2011).
- [24] [CMS Collaboration], CMS-PAS-HIG-11-025, CMS-PAS-HIG-11-029, CMS-PAS-HIG-11-030, CMS-PAS-HIG-11-031, CMS-PAS-HIG-11-032; Chatrchyan, S., *et al.*, Phys. Lett. B 699, 25 (2011).
- [25] Aprile, E., *et al.* [XENON100 Collaboration], Phys. Rev. Lett. 105, 131302 (2010) (arXiv:1005.0380 [astro-ph.CO]); arXiv:1005.2615 [astro-ph.CO].
- [26] Bernabei, R., *et al.* [DAMA Collaboration], Eur. Phys. J. C 67, 39 (2010) [arXiv:1002.1028 [astro-ph.GA]]; Eur. Phys. J. C 56, 333 (2008) [arXiv:0804.2741 [astro-ph]].
- [27] Cai, Y., He, X.G., and Ren, B., arXiv:1102.1522 [hep-ph].
- [28] Asano, M., and Kitano, R., Phys. Rev. D 81, 054506 (2010).

- [29] Eidelman, S., *et al.*, Phys. Lett. B592, 1 (2004).
- [30] Nason, P., Phys. Lett. B 175, 223 (1986).
- [31] Chivukula, R.S., Cohen, A.G., Georgi, H., Grinstein, B., and Manohar, A.V., Ann. Phys. 192, 93 (1989).
- [32] Voloshin, M.B., Sov. J. Nucl. Phys. 44, 478 (1986) [Yad. Fiz. 44, 738 (1986)].
- [33] Gunion, J.F., Haber, H.E., Kane, G., and Dawson, S., '*The Higgs Hunters Guide*', Perseus Publishing, Cambridge, MA, (1990).
- [34] McKeen, D., Phys. Rev. D 79, 015007 (2009).
- [35] Djouadi, A., Phys. Rept. 459, 1 (2008).
- [36] Love, W., *et al.*, Phys. Rev. Lett. 101, 151802 (2008).
- [37] Anastassov, A., *et al.* [CLEO Collaboration], Phys. Rev. Lett. 82, 286 (1999).
- [38] Athar, S.B., *et al.* [CLEO Collaboration], Phys. Rev. D 73, 032001 (2006).
- [39] Auber, B., *et al.* [BABAR Collaboration], Phys. Rev. Lett. 103, 081803 (2009).
- [40] Bartsch, M., Beylich, M., Buchalla, G., and Gao, D.N., JHEP 0911, 011 (2009).
- [41] Chen, K.F., *et al.* [BELLE Collaboration], Phys. Rev. Lett. 99, 221802 (2007).
- [42] Buras, A.G., Acta Phys. Polon. B 41, 2487 (2010).
- [43] The CMS and LHCb Collaborations, LHCb-CONF-2011- 047, CMS PAS BPH-11-019.
- [44] Low, I., Schwaller, P., Shaughnessy, G., and Wagner, C.E.M., arXiv:1110.4405 [hep-ph]. Note that in deriving the constraint on the invisible width of the simplest singlet dark-matter model, the authors have used the ATLAS and CMS older analysis available at that time. Using the latest analysis [23, 24] will rule out the possibility of opening up the Higgs window above 140GeV in the one singlet model.
- [45] Abada, A., and Nasri, S., work in progress.